FULL PAPER

Enhanced Crystallization by Methanol Additive in Anti-solvent for Achieving High-quality $MAPbI_3$ Perovskite Films in Humid Atmosphere

Fu Yang*, Muhammad Akmal Kamarudin, Putao Zhang, Gaurav Kapil, Tingli Ma, Shuzi Hayase*

Abstract: Perovskite solar cells have attracted considerable attention owing to easy and low-cost solution manufacturing process with high power conversion efficiency. However, the fabrication process is usually performed inside glovebox to avoid the moisture, as organometallic halide perovskite is easily dissolved in water. In this study, we propose one-step fabrication of high-quality $MAPbI_3$ perovskite films in around 50 % RH humid ambient air by using diethyl ether as an anti-solvent and methanol as an additive into this anti-solvent. Because of the existence of methanol, the water molecules can be efficiently removed from the gaps of perovskite precursors and the perovskite film formation can be slightly controlled leading to pinhole-free and low roughness film. Concurrently, methanol can modify a proper DMSO ratio in the intermediate perovskite phase to regulate perovskite formation. Planar solar cells fabricated by using this method exhibited the best efficiency of 16.4 % with a reduced current density-voltage hysteresis. This efficiency value is approximately 160 % higher than the devices fabrication by using only diethyl ether treatment. From the impedance measurement, it is also found that the recombination reaction has been suppressed when the device prepared with additive anti-solvent way. This method presents a new path for controlling the growth and morphology of perovskite films in the humid climates and uncontrolled laboratories.

Introduction

The efficiency of organometallic halide perovskite solar cells (PSCs) has increased from 3.8 % to more than 22 %, due to their super charge carrier mobility, high absorption coefficient and band gaps close to Shockley-Queisser limit.[1] Besides the remarkable photovoltaic performance, anti-solvent assisted one-step spin coating crystallization method is one of the widely used methods to achieve high quality perovskite film.[2] These superior characteristics is attributed to the high crystallinity of the perovskite material which can be prepared using one-step method with anti-solvent process. Perovskite intermediate phase is formed when the anti-solvent is dropped during the spin-coating process where the evaporation rate of the solvent determines the film thickness after which the solution becomes supersaturated, leading to nucleation and finally crystal growth. The anti-solvent is responsible for controlling the morphology of the perovskite material by inducing fast precipitation of perovskite resulting in highly dense and smooth perovskite film. Typically used anti-solvents are diethyl ether,[3] toluene,[4] chlorobenzene[5] and ethyl acetate[6] which have low boiling point, a weak electron donating capability and a poor coordination ability with perovskite precursors. The week coordination of the anti-solvents can modify the balance between the reduction of grain boundaries and the adjustment of the perovskite films.[7] Therefore, it is important to study the effect of the anti-solvent in coordinating perovskite crystal growth and film formation as the choice of the anti-solvent affects the overall morphology and hence the optoelectronic performance of the perovskite layer. In addition, the fabrication process of PSCs is usually performed inside nitrogen/argon filled glovebox to avoid moisture, as perovskite layer can degrade easily in the ambient humidity condition.[8] Moreover, it was reported that it was difficult to get a high-quality perovskite film by using diethyl ether, chlorobenzene or toluene as the anti-solvent in the humid ambient air.[6a] Thus, it is significant chanlengeful and meaningful to prepare high-quality perovskite films in the humid ambient air. Yan group used lead (II) thiocyanate ($Pb(SCN)_2$) to increase the humidity resistance for preparation of $MAPbI_{3-x}SCN_x$ perovskite film in more than 70 % relative humidity (RH) showing efficiency up to 15 %.[9] By employing the assistance of hydrochloric acid to accelerate $MAPbI_3$ perovskite film formation, Zhao et al prepared high quality MAPbI3 perovskite films which showing efficiency of 14.76 % in about 60 % RH air condition.[10] Watson and his group reported ethyl acetate as an anti-solvent to prepare pinhole-free MAPbI3 perovskite films with efficiency of 14.5 % in 75 % RH air atmosphere, where ethyl acetate acts as a moisture absorber protecting sensitive perovskite intermediate phases from water molecules during film formation and annealing.[6a] However, there are still quite few reports on deposition of perovskite films in the high humidity ambient air condition.

Generally, the morphology of perovskite film could be enhanced by controlling growth and crystallization of the perovskite.[11] There are many reports about the perovskite crystallinity enhancement by adding some additives into perovskite precursor solution, which lead to an increased photovoltaic performance of

[a] F. Yang, Dr. M. A. Kamarudin, P. T. Zhang, Dr. G. Kapil, Prof. Dr. T. L. Ma, Prof. Dr. S. Hayase
Graduate School of Life Science and Systems Engineering
Institution Kyushu Institute of Technology
2-4 Hibikino Wakamatsu-ku, Kitakyushu 808-0196, Japan
E-mail: yang-fu@edu.life.kyutech.ac.jp; hayase@life.kyutech.ac.jp

Supporting information for this article is given via a link at the end of the document.

the solar cell devices.[12] Moreover, high performance perovskite solar cells need to be fabricated inside glovebox to avoid moisture, as organometallic halide perovskite is easily dissolved and degrade in water. A dry atmosphere slightly raises the costs of fabrication of PSCs, while the ambient air can significantly simplify fabrication processes, reduce costs and move forward commercial production of PSCs. However, as far as we know, there is no report revealing the influence of additive into anti-solvent on perovskite crystal growth and film formation in the humid ambient air.

In this work, we employed methanol as an additive in diethyl ether to control the morphology and investigate the growth mechanism of $MAPbI_3$ perovskite films using one-step fabrication process in high humidity atmosphere. Compared to diethyl ether, the methanol additive anti-solvent has a stronger solubility of water and dimethyl sulfoxide (DMSO), which plays a critical role in preparing high density, pinhole-free and uniform $MAPbI_3$ perovskite film as evidenced from scanning electron microscope image and atomic force microscopy. When increasing the ratio of methanol in diethyl ether, the water resistance of perovskite is enhanced, which results in a high quality and pinhole-free perovskite film. In addition, methanol can modify a proper DMSO ratio to form in the intermediate perovskite phase accelerating perovskite crystal formation. The best solar cells exhibited PCE of 16.4 % prepared with 3 % additive anti-solvent, which is approximately 160 % higher than the devices fabricated using diethyl ether without methanol additive. We believe that this additive anti-solvent method would be useful for understanding the formation mechanism of perovskite layer and indicate a desirable direction for PSCs fabrication in humid and uncontrolled condition.

Results and Discussion

Figure 1a shows the X-ray diffraction (XRD) patterns of perovskite films prepared on glass substrates by different ratio methanol in the diethyl ether (0 %, 1 %, 2 %, 3 %, 4 %). Strong diffraction peaks locate at 14.1°, 28.4°, 31.9°, 40.7° and 43.1° for 2θ scan are observed, corresponding to the planes of (110), (220), (222), (224) and (314) of perovskite which are in agreement with previous reports.[13] Therefore, we can make sure from the XRD results that the perovskite films are highly crystallized perovskite phase. In addition, a weak diffraction peak of PbI_2 appeared at 12.7°, where the intensity of the peak increased upon higher methanol ratio. This increment of PbI_2 concentration could be ascribed to the high solubility of methylammonium iodide (MAI) in methanol in which the methylammonium component is removed from the perovskite structure leaving behind PbI_2.[14] It is noticed that (110) peaks shifted to the left (**Figure 1b**) when compared to the control sample, suggesting that the crystallites are experiencing homogenous strain as there was only peak shift but not peak broadening.[15] **Figure 1c** shows the UV-vis absorption spectra of the different perovskite samples. The absorbance increased upon addition of methanol reaching the highest absorbance at 3% methanol concentration and then started to decrease when more methanol is added. This is mainly due to improved surface coverage and reduction of pinholes of the perovskite thin film. [16]

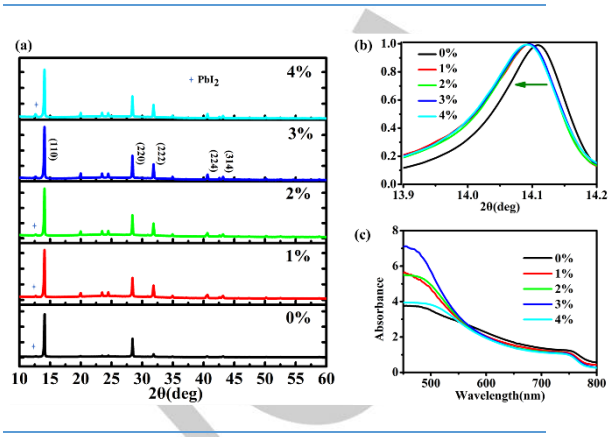

Figure 1. (a) XRD of $MAPbI_3$ films on glass substrates prepared by different methanol additive in diethyl ether (0%, 1%, 2%, 3%, 4%). (b) Normalized XRD plot of (110) peak. (c) UV-vis absorption spectra of perovskite films prepared by various concentration of additive anti-solvent.

Figure 2 shows the surface morphology of annealed $MAPbI_3$ perovskite films prepared by different methanol additive ratio anti-solvent by SEM. With diethyl ether, it can be seen the crystals are badly formed with the presence of pinholes. When 1 % addition of methanol, similar morphology was observed. However, adding 2 % and more methanol changed the morphology significantly. The crystallinity of the perovskite sample was improved in which the size distribution is homogenous throughout the sample in addition to the reduction of pinholes. The largest crystal size was obtained with the sample prepared using 4 % methanol although there was a big inhomogeneity in size between grains. The statistical result of grain size of the film has been summarized in **Figure S2**, with an average grain size of 240 nm for 2 % additive anti-solvent, 340 nm for 3 % additive anti-solvent, and 280 nm for 4 % additive anti-solvent. For the 0 % and 1 % additive anti-solvent sample, the average size could not be determined due to the poorly formed crystals.

Figure 3 shows the AFM images of perovskite film prepared by different methanol ratio additive anti-solvent. The Rq roughness values were measured to be 26.9, 23.1, 11.6, 10.4 and 10.1 for samples prepared by different methanol content of 0 %, 1 %, 2 %, 3 % and 4 %, respectively. The decreased roughness from methanol content from 0 % to 4 % supports the data obtained from SEM images in which high quality with improved surface morphology is obtained with methanol addition. The 3D surface images shown in **Figure 3 b, d, f, h, j** clearly shows the decrease of surface roughness of the perovskite films. It is expected that these improvements will be reflected at the perovskite/Spiro-OMeTAD interface which could enhance the performance of the solar cells.

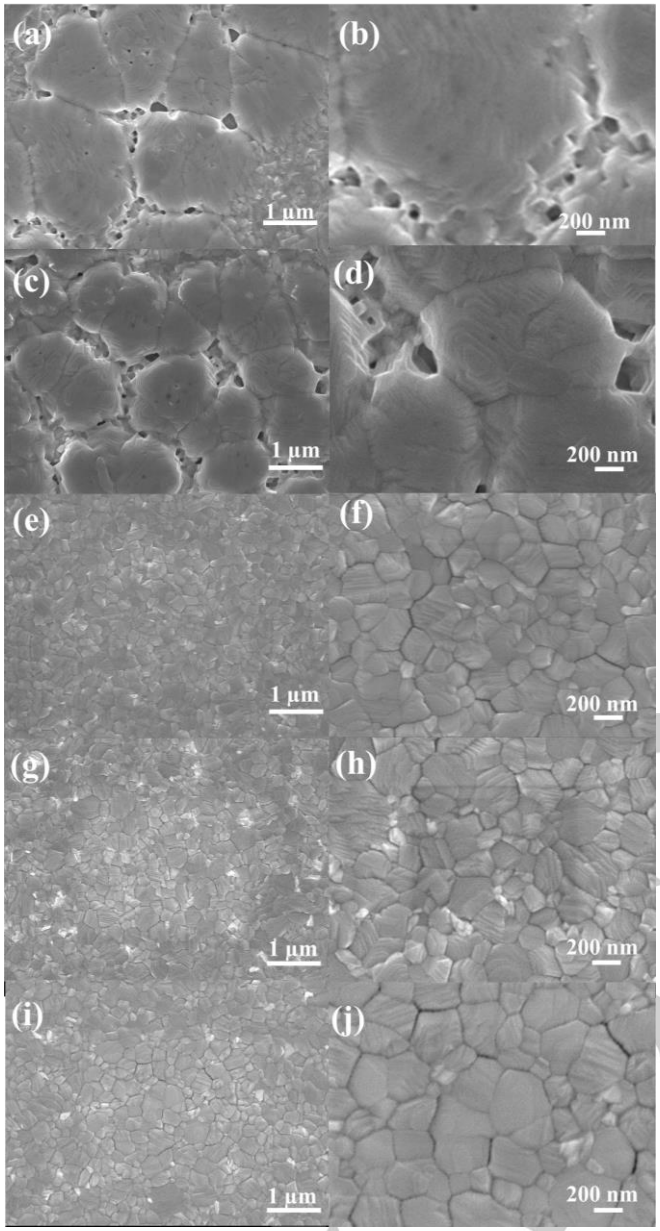

Figure 2. SEM images of annealed $MAPbI_3$ perovskite film on FTO substrates prepared by different methanol content in diethyl ether. (a) (b) 0 %; (c) (d) 1 %; (e) (f) 2 %; (g) (h) 3 %; (i) (j) 4 %.

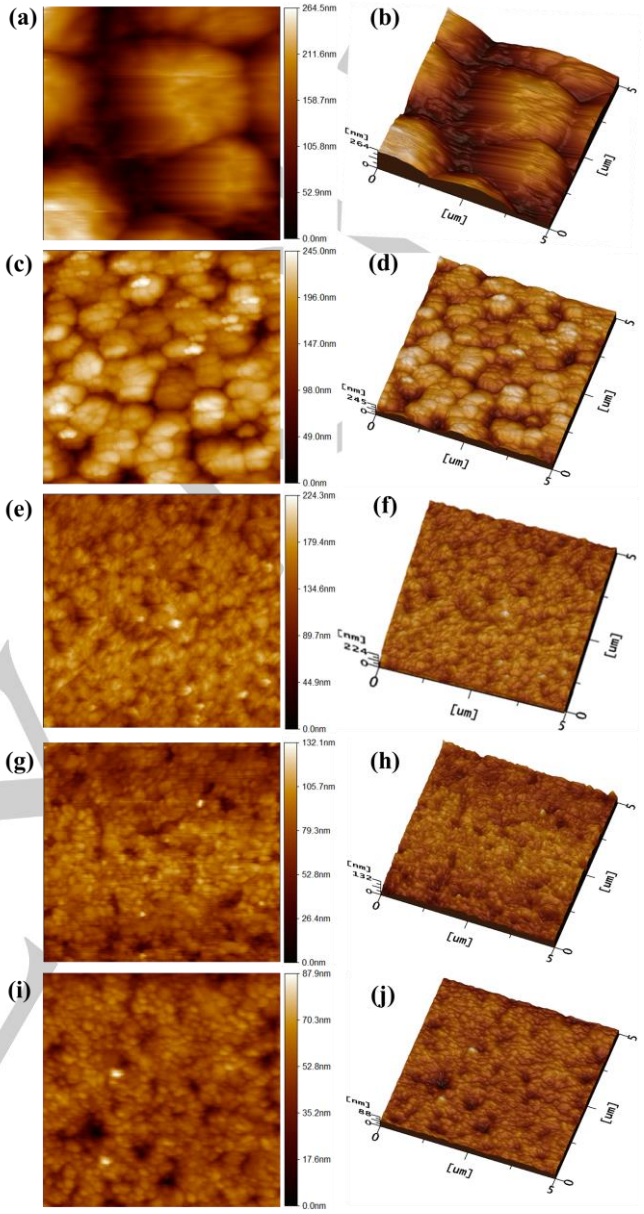

Figure 3. AFM images (a, c, e, g, i) and the corresponding 3D surface plot images (b, d, f, h, j) of $MAPbI_3$ films prepared by different methanol additive content anti-solvent. (a) (b) 0 %; (c) (d) 1 %; (e) (f) 2 %; (g) (h) 3 %; (i) (j) 4 %.

Figure 4 shows FTIR spectra of perovskite films prior to annealing prepared by various methanol concentration in the additive anti-solvent (0 %, 1 %, 2 %, 3 %, 4 %). The films of perovskite intermediate phase demonstrated similar peak positions. The S–O stretching vibration and N–H stretching vibration are located at 1020 cm^{-1} and around 3190 cm^{-1}, respectively, as shown in **Figure 4a**.[17] The N-H peak shifted to long wavenumber when N-H bond coordinated to DMSO, implying that an intermediate phase of MAI-PbI_2-DMSO has been formed.[18] The N-H peak of the intermediate phase is at 3190 cm^{-1} for 0 % methanol concentration in the additive anti-solvent, 2189 cm^{-1} for 1 %

methanol additive , 3184 cm^{-1} for 2 % methanol additive , 3181 cm^{-1} for 3 % methanol additive and 3179 cm^{-1} for 4 % methanol additive . This means that amount of DMSO is extracted by the additive anti-solvent method. In addition, the change of DMSO concentration in the intermediate phase can be deduced by calculating the ratio of S-O intensity peak at 1020 cm^{-1} to N-H intensity peak at around 3190 cm^{-1} shown in **Figure 4c**. The ratio decreased from 1.32, 1.08, 1.05, and 1.04 to 1.02 as the methanol content is increased. Park et al. reported that excessive amount of DMSO in the perovskite intermediate phase would lead to an inhomogeneous perovskite film because of the gradual vaporization of DMSO from the perovskite film.[3] In addition, the less DMSO in the intermediate phase also means that the time needed for the phase change from perovskite intermediate phase to perovskite film is accelerated.[19] Inversely, excessive amount of DMSO in the intermediate phase also lead to inhomogeneous perovskite film with small grain size. Therefore, by adjusting the methanol ratio in the additive anti-solvent, a proper amount of DMSO into the perovskite intermediate phase can be controlled to assist crystallization leading to a pinhole-free homogenous perovskite film.

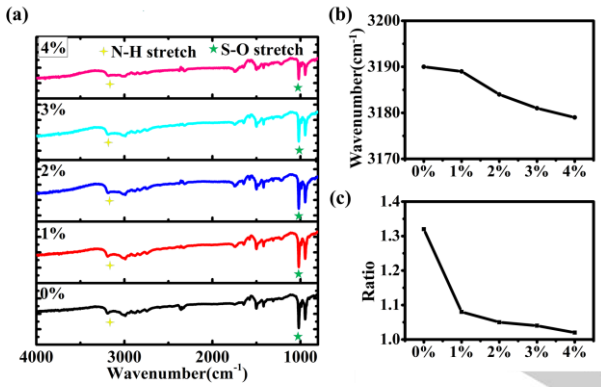

Figure 4. (a) Attenuated Total Reflectance FTIR spectra of $MAPbI_3$ films (on Pt substrates) prepared by different methanol concentration additive anti-solvent (0%, 1%, 2%, 3%, 4%). (b) The N-H stretch peak position of the non-annealed film by different methanol additive anti-solvent. (c) Ratio of intensity of absorbance at 1020 cm-1 to 3190 cm-1 (1020 cm-1: 3190 cm-1).

In the anti-solvent based one-step preparation process, the perovskite layer is formed by spin coating of the precursor solution followed by thermal annealing. This preparation process usually has two stages. In the first stage, the liquid film is thinning by centrifugal forces. After a transition point, evaporation rate of the solvent dominates the film thinning, which depends on the vapor pressure of the solvent. Then at the second stage, solution becomes supersaturated, nucleation occurs leading to crystal growth and solid intermediate (or perovskite) film forms. Thus, in order to prepare high-quality perovskite film, the important stage is to accelerate the evaporation rate of excess DMF and control the perovskite crystallization process.[20] For two immiscible solvents, the total vapor pressure of the mixed solution is close to the sum of the two solvents' vapor pressures, and the boiling point of the mixture should be lower than of each solvent.[21] Following this rule, introducing the high vapor pressure anti-solvent for one-step preparing perovskite film will help to promote a uniform and high-quality film. In addition, after the perovskite intermediate phase formed in the humid air atmosphere, it is better to reduce contact time of this intermediate phase with the moisture within the air to avoid degradation by the water. Therefore, the second way is to speed up the perovskite nucleus growth rate to reduce the formation time of perovskite intermediate phase to perovskite. **Figure 5** shows the schematic diagram representing the perovskite crystal growth mechanism between pure diethyl ether and the additive anti-solvent. It is known that diethyl ether has high vapor pressure (71.8 Kpa at 25 °C) and is immiscible in both DMSO and water (1.5 vol% of water). [22] However, DMSO, water and methanol are mutual miscible. During the normal diethyl ether anti-solvent process, diethyl ether quickly extracts DMF from the perovskite film. As the same time, perovskite and perovskite precursors are insoluble in diethyl ether. Therefore, after diethyl ether extracting the solvents from the perovskite film in the washing process, some water from the humid air atmosphere remains on the wet MAI-PbI_2-DMSO perovskite intermediate film before annealing and can only be removed upon heating above 100 °C. Hence, an inhomogeneous film with many pinholes and rough surface is formed, which was proved by the SEM image of **Figure 2a**. When methanol is added into the diethyl ether, methanol removes the residual water quickly through its infinite solubility with water, which lead to a pinhole-free homogeneous film with a smoother surface, shown in SEM image of **Figure 2g**. Meanwhile, methanol could also remove redundant DMSO from the perovskite intermediate phase to accelerate the perovskite formation as methanol can slightly dissolve DMSO, which was proved by the FTIR spectra in **Figure 4**. It is suggested a proper intermediate phase is a key point for preparing the perovskite layer with desirable morphology.[23] Thus, an optimum methanol concentration can extract suitable amount of DMSO content from the precursor solutions to accelerate the perovskite formation and give an appropriate MAI-PbI_2-DMSO intermediate phase. On the other hand, in the perovskite film growth process, the crystal grain growth rate is determined by the Gibbs free energy, which includes chemical energy difference, surface energy and interface energy of the grains. Acik and co-workers have proposed that the overall Gibbs free energy was lower when using alcohols (including methanol) to catalyze the growth of $MAPbI_3$ crystals.[24] In common homogenous nucleation, the relationship of overall Gibbs free energy change (ΔG) and nucleus radius (r) can be given as the equation:[25]

$$\Delta G(r) = -\frac{4\pi r^3}{3V_M} RT \ln(S) + 4\pi r^2 \gamma$$

where R, T, S, γ and V_M represent gas constant, absolute temperature, supersaturation ratio, energy of liquid-crystalline nucleus interface and nucleus` molar volume, respectively. **Figure 6b** and **6d** schematically depict the Gibbs free energy diagrams as a function of nuclei radius in case of the anti-solvent treatment without or with methanol additive. When methanol is used as an additive in the anti-solvent for preparing the perovskite film, the Gibbs free energy is lower than that of without methanol additive because of the chemical heterogeneity effect.[26] As a

result, more nuclei are formed, which lead to the small size grain growth, shown in **Figure 2c**.

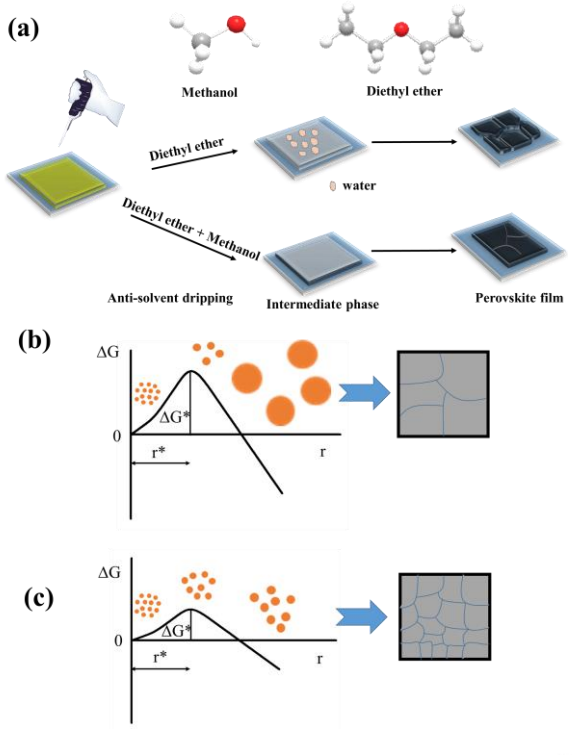

Figure 5. (a) Schematic diagram of anti-solvent step using diethyl ether and methanol additive diethyl ether. (b) Gibbs free energy diagrams for nucleation and growth of $MAPbI_3$ perovskite film by diethyl ether anti-solvent. (c) Gibbs free energy diagrams for nucleation and growth of $MAPbI_3$ perovskite film by methanol additive diethyl ether anti-solvent.

The effect of methanol additive into diethyl ether anti-solvent method on solar cells performance was investigated via planar FTO/SnO_2/$MAPbI_3$/Spiro/Au perovskite solar cells. Devices were fabricated under around 50 % RH humid air condition. **Figure 6a**, **6b** illustrates the schematic structure and energy diagram of the PSCs. **Figure 6c** shows the J−V curves of devices prepared with various methanol concentration in the additive anti-solvent. The measured photovoltaic parameters of the champion the different devices are listed in **Table 1**. Device prepared using only diethyl ether showed the lowest power conversion efficiency of 6.3 % mainly due to the low V_{OC}. Upon addition of methanol into the anti-solvent, there is an increasing trend of all the parameters of PSCs. The most efficient device was prepared by 3 % methanol additive anti-solvent, with a champion PCE of 16.4 %, J_{sc} of 22.48 mA/cm^2, V_{OC} of 1.04 V, and FF of 70.0 %. The efficiency value is approximately 160 % higher than the cell fabricated using pure diethyl ether as anti-solvent treatment. The obtained JSC follows the same trend as the UV-Vis absorption spectra in which 3 % sample has the highest absorption followed by 2 %, 4%, 1 % and finally 0 %. The high absorptance resulted in higher number of photons being absorbed by the perovskite active layer and be converted into electrons. The calculated J_{SC} is obtained by integrating the IPCE curve shown in **Figure 7d**. The value obtained is in agreement with the measured value from the J-V curve. **Figure S3** demonstrates the J-V curve of reverse and forward direction for each type of device. **Figure S4** shows the photovoltaic statistics for the planar PSCs prepared by different additive anti-solvent condition.

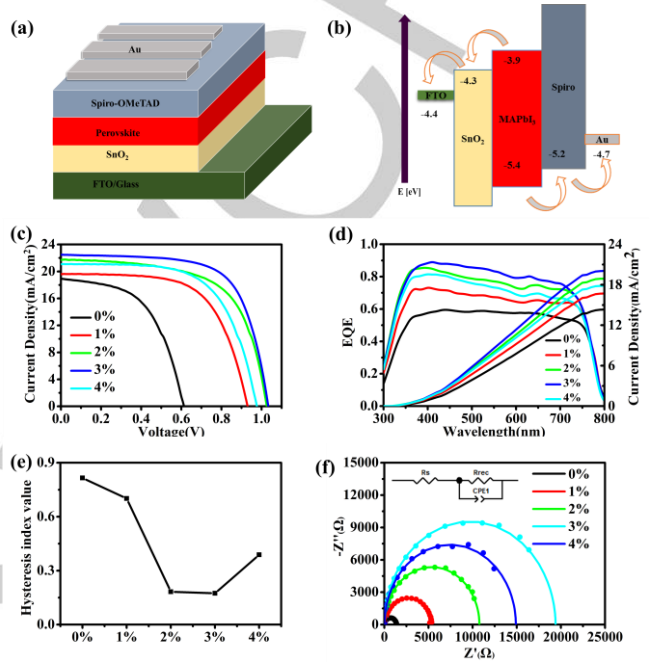

Figure 6. Schematic structure (a) and (b) energy diagram of the planar FTO/SnO_2/ $MAPbI_3$/Spiro-OMeTAD/Au planar perovskite solar cells. (c) J−V curves of the control and additive anti-solvent as anti-solvent treated devices measured under illumination of an AM 1.5 solar simulator (100 mWcm $^{-2}$) in air. The scanning direction is from open-circuit voltage to short-circuit current (reverse). (d) EQE spectra of the control and additive anti-solvent as anti-solvent treated devices measured in air. (e) Hysteresis index value calculated from the J-V curves; (f) The Nyquist plots of different condition additive anti-solvent based planar champion devices measured in the dark under 0.7 V applied bias and the equivalent circuit diagram, the fitted curves and the experimental data are shown as solid lines corresponding points, respectively. (a) Attenuated Total Reflectance FTIR spectra of $MAPbI_3$ films (on Pt substrates) prepared by different methanol concentration additive anti-solvent (0 %, 1 %, 2 %, 3 %, 4 %). (b) The N-H stretch peak position of the non-annealed film by different methanol additive anti-solvent. (c) Ratio of intensity of absorbance at 1020 cm^{-1} to 3190 cm^{-1} (1020 cm^{-1}: 3190 cm^{-1}).

In order to compare the quality of the perovskite layers and hence the PSCs, the hysteresis index (HI) value was calculated.[27] The HI value was 0.81 for 0 % methanol additive, 0.70 for 1 % methanol additive, 0.18 for 2 % methanol additive, 0.17 for 3 % methanol additive, and 0.38 for 4 % methanol additive, respectively which means the hysteresis of PSCs decreased an the methanol content increased. There are many reports analyzing the origin of hysteresis in perovskite solar cells such as ionic motions within perovskite, charge trapping and de-trapping due to crystal defects and band bending between the different interfaces. Such low HI index could be attributed to the uniform growth of the $MAPbI_3$ layer obtained by additive anti-solvent

deposition process, effectively reducing the presence of grain boundaries and thus charge transfer between grains are more efficient. To investigate the charge transfer mechanism at the interfaces, electrochemical impedance spectroscopy (EIS) measurement was performed. The Nyquist plots of PSC devices are shown in **Figure 6f** where the illustrated equivalent circuit diagram was used to fit the plot. Here, one semicircle is seen at high frequency corresponding to the charge transport at the back electrode and hole transporting material (HTM) as reported previously.[28] From **Figure 6f**, the same trend as the J-V curve is observed with the Nyquist plot where the sample prepared with 3 % methanol additive anti-solvent has the highest recombination resistance (R_{rec}) as determined from the width of the semicircle and decreased when less methanol content was employed. The large R_{rec} suggests that the electron-hole recombination is suppressed at the $MAPbI_3$/Spiro interface due to better interfacial contact because of the pinhole-free perovskite layer. This allows for efficient charge extraction at both the electron and hole transporting materials.

Table 1. Photovoltaic parameters of champion planar PSCs devices.

Condition[a]	J_{sc} (mA/cm^2)	Voc (V)	FF (%)	PCE (%)
0%	18.93	0.61	53.9	6.3
1%	19.60	0.93	63.4	11.6
2%	21.71	1.03	63.5	14.2
3%	22.48	1.04	70.0	16.4
4%	21.06	0.98	63.4	13.1

[a] The ratio of different methanol concentration in diethyl ether (0%, 1%, 2%, 3%, 4%).

Upon addition of a small amount of methanol into the anti-solvent, it is assumed that the water retention of the additive anti-solvent is enhanced compared to pure diethyl ether. To confirm this hypothesis, deionized water was deliberately added to the anhydrous diethyl ether and 3 % methanol additive anti-solvent. **Figure 7** shows the SEM images of perovskite films fabricated with different water content added to diethyl ether and 3 % methanol additive anti-solvent. In the case of 0.5 % volume water added to pure diethyl ether, the formation of more pinholes was observed as shown in **Figure 7a**. This is due to more water molecules present in the perovskite intermediate phase during crystal growth. However, the 3 % additive anti-solvent contaminated with even 1 % water exhibited crystalline and a pinhole-free surface which is due to the miscibility of water in methanol and thus the water molecules are extracted together with methanol. Furthermore, planar perovskite solar cells were prepared by 3 % additive anti-solvent contaminated with 0.5 % and 1 % water, shown in **Figure S5**. For 0.5 % water in 3% additive methanol anti-solvent treatment device, we can get the PCE up to 14.3%. And for 1 % water in 3% additive methanol anti-solvent treatment device, the champion PCE was 12.3%. However, for the 0.5 % water in only diethyl ether anti-solvent, the champion PCE is just 4.6 %. Those results mean that disadvantage in the presence of moisture (water) can be limited by utilizing the methanol additive anti-solvent method.

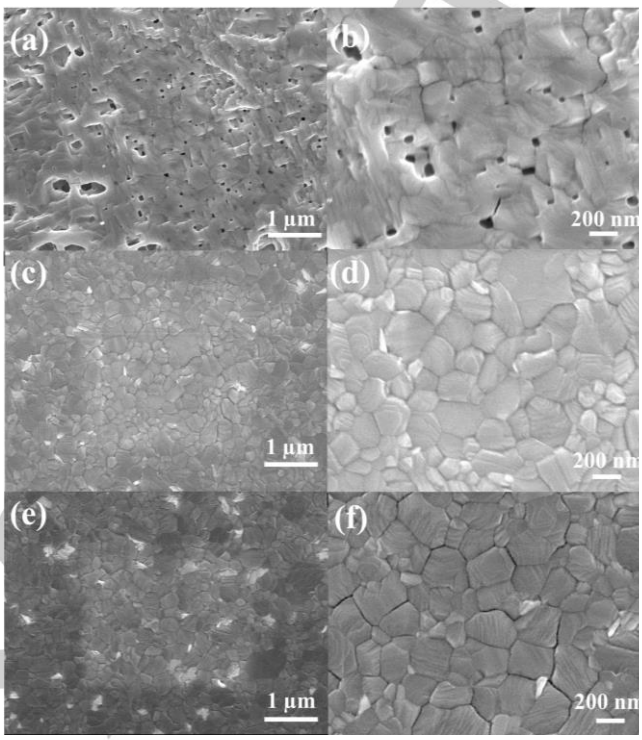

Figure 7. SEM images of annealed $MAPbI_3$ perovskite film on FTO substrates by water contaminated additive anti-solvent. (a) (b) 0.5 % water in diethyl ether; (c) (d) 0.5 % water in 3 % methanol additive anti-solvent; (e) (f) 1 % water in 3 % methanol additive anti-solvent.

To further investigate universality of the additive method, other alcohols including ethanol, 2-propanol and 1-butanol were used as the additive into diethyl ether anti-solvent for preparing MAPbI3 perovskite films and solar cells. An interesting observation is that when increasing the alcohol additive content in diethyl ether, similar results as in the case of methanol additive were achieved. With the raise of alcohol` content, the perovskite film showed less pinholes, shown in **Figure S7**. Pinhole free perovskite films were obtained by 5% ethanol, 8% 2-propanol and 12% 1-butanol, respectively, shown in **Figure 8**. Then planar solar cells were prepared by 5% ethanol, 8% 2-propanol and 12% 1-butanol additive in diethyl ether anti-solvent. The champion device for 5% ethanol additive anti-solvent is 15.4%, for 8% 2-propanol additive anti-solvent is 14.8% and for 12% 1-butanol additive is 15.2 %, shown in **Figure S8**. Those results demonstrated that the additive method is a universal method for preparing the high quality perovskite films in the humid air atmosphere. Therefore, from the above discussion, we can draw the conclusion that alcohols additive in diethyl ether will be a good direction for the fabrication of high performing perovskite solar cells in humid

ambient atmosphere which is beneficial from the low-cost and mass-production point of view.

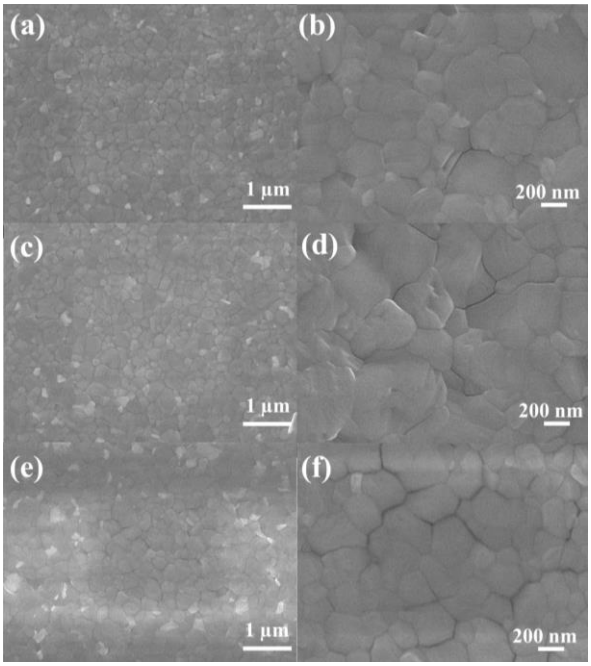

Figure 8. SEM images of annealed $MAPbI_3$ perovskite film on FTO substrates by by different kind of alcohol additive anti-solvent. (a) (b) 5% ethanol additive in diethyl ether; (c) (d) 8 % 2-propanol additive in diethyl ether anti-solvent; (e) (f) 12 % 1-butanol additive in diethyl ether anti-solvent.

Conclusions

In conclusion, high performing planar $MAPbI_3$ perovskite solar cells has been fabricated at high relative humidity (around 50 % RH) using methanol additive into diethyl ether anti-solvent. The highest solar cell efficiency was obtained with perovskite layer prepared with 3 % methanol in diethyl ether showing a PCE of 16.4 %, V_{oc} of 1.04 V, J_{sc} of 22.48 mA/cm^2, and FF of 70.0 %. The reason for this high performing device can be attributed to the formation of dense perovskite film with smooth surface due to fast extraction of water molecules during annealing as methanol has high water solubility. This has been proved experimentally by deliberately adding water into the perovskite precursor solution and prepared the perovskite solar cells using 3 % methanol-diethyl ether anti-solvent. Despite the addition of water in the precursor solution, the film still showed highly crystalline and smooth surface morphology. Additionally, addition of methanol can provide the optimum DMSO content in the intermediate perovskite phase to accelerate perovskite formation. Moreover, due to the improved interfacial contact of the highly crystalline perovskite, the hysteresis issue has been improved together with the reduction of electron-hole recombination reaction as seen from the impedance measurement. Furthermore other alcohols including ethanol, 2-propanol and 1-butanol were tried as the additive into diethyl ether similarly worked as well, which proved the universal usage of the additive into anti-solvent method. This work provides a good direction for the fabrication of high performing perovskite solar cells at high humidity ambient atmosphere which is beneficial from the low-cost and mass-production point of view.

Experimental Section

Preparation of perovskite solar cells

All reagents including diethyl ether (Aldrich, 99.8 %) and methanol (Wako, 99.5 %) were used without further purification. For preparing the additive ant-solvent, different volume methanol was added in diethyl ether, i. e 60 µl methanol was added in 2 mL diethyl ether for getting 3% methanol additive anti-solvent. F-doped SnO_2 (FTO glass, Nippon Sheet Glass Co. Ltd) substrates were first patterned and cleaned using zinc powder and 6 N hydrochloric acid solution. Tin (II) chloride (Aldrich, 98 %) was dissolved in ethanol (Wako, 99.8 %) to form 0.1 M SnCl2 solution. Then the SnCl2 solution was spin-coated on the cleaned FTO glass at 2000 rpm for 30 seconds.[29] The substrate was annealed at 180 °C for 60 minutes on a hot plate to form a dense SnO_2 electron transport layer. Equal molar ratio of MAI (TCI, 98 %) and PbI_2 (TCI, 99.99 %) were dissolved in anhydrous dimethylformamide (DMF, Aldrich, 99.8 %) and anhydrous dimethyl sulfoxide (DMSO, Aldrich, 99.8 %) (DMF: DMSO, 4:1) to prepare 1.5 M $MAPbI_3$ precursor solution and stirred at room temperature for 1 hour. The perovskite precursor solution was spin-coated on SnO_2-coated substrate at 4000 rpm for 25 seconds and the anti-solvent (0.5 ml) was dripped on the substrate 10 seconds after starting the spin-coating process, followed by heating at 100 °C for 10 minutes. The Spiro-MeOTAD layer was prepared by spin-coating a chlorobenzene solution containing 180 mM Spiro-MeOTAD (Aldrich, 99 %), 60 mM tert-butylpyridine (Aldrich, 96 %), 30 mM Li-TFSI (Aldrich, 99.95 %) (520 mg/mL in acetonitrile) and 33 mM FK209 (Aldrich, 99 %) (300 mg/mL in acetonitrile) at 4000 rpm for 30 seconds. Finally, 80 nm-thick Au counter electrode was deposited by thermal evaporation. All procedures were performed at around 50 % relative humidity in ambient air condition (Relative humidity was recorded using a hygrometer accurate to ± 5 % RH between 25 % and 69.9 % RH, ±10 % RH between 70 % and 90 % RH) (A&D Company, AD-5681)).

Characterization

Solar cell performance was measured by a solar simulator (CEP-2000SRR, Bunkoukeiki Inc., AM 1.5G 100 mWcm^{-2}) and a mask with exposure area 0.10 cm^2 was used during the photovoltaic measurements with a 0.1 V/s scanning rate in reverse (from the open-circuit voltage (Voc) to the short-current density (Jsc)) and forward (from Jsc to Voc) modes under standard global AM 1.5 illumination. The IPCE spectra were recorded using a monochromatic Xenon lamp (Bunkouki CEP-2000SRR). X-ray Diffraction (XRD) Study. The surface morphology of the samples was observed through a scanning electron microscope (SEM) (JEOL, Neoscope, JCM-6000) and a Bruker Innova atomic force microscopy (AFM) (JSPM-5200). Attenuated Total Reflectance Fourier transform IR spectras (FT-IR) were tested by FT-IR spectrometer (JASCO, FT/IR-4100 Series) via an attenuated total reflectance (ATR) crystal. The XRD patterns were obtained by a Rigaku Smartlab X-ray diffractometer with monochromatic Cu-Kβ

irradiation (45 kV/200 mA). The UV-Vis measurement was performed using a JASCO V-670. Spectrophotometer. Electrochemical impedance spectroscopic (EIS) measurements were performed in the dark using an electrochemical workstation with a frequency range from 1 Hz to 1 MHz at 0.7 V applied bias.

Keywords: perovskite solar cell • anti-solvent • humid atmosphere • $MAPbI_3$ • Planar

[1] a) M. M. Lee, J. Teuscher, T. Miyasaka, T. N. Murakami, H. J. Snaith, Science 2012, 338, 643-647; b) T. Leijtens, G. E. Eperon, S. Pathak, A. Abate, M. M. Lee, H. J. Snaith, Nature communications 2013, 4, 2885; c) S. D. Stranks, G. E. Eperon, G. Grancini, C. Menelaou, M. J. Alcocer, T. Leijtens, L. M. Herz, A. Petrozza, H. J. Snaith, Science 2013, 342, 341-344; d) A. Kojima, K. Teshima, Y. Shirai, T. Miyasaka, Journal of the American Chemical Society 2009, 131, 6050-6051; e) W. S. Yang, B.-W. Park, E. H. Jung, N. J. Jeon, Y. C. Kim, D. U. Lee, S. S. Shin, J. Seo, E. K. Kim, J. H. Noh, Science 2017, 356, 1376-1379; f) W. Shockley, H. J. Queisser, Journal of applied physics 1961, 32, 510-519.
[2] M. Konstantakou, D. Perganti, P. Falaras, T. Stergiopoulos, Crystals 2017, 7, 291.
[3] N. Ahn, D.-Y. Son, I.-H. Jang, S. M. Kang, M. Choi, N.-G. Park, Journal of the American Chemical Society 2015, 137, 8696-8699.
[4] N. J. Jeon, J. H. Noh, Y. C. Kim, W. S. Yang, S. Ryu, S. I. Seok, Nature materials 2014, 13, 897-903.
[5] a) C. Liu, Y. Yang, Y. Ding, J. Xu, X. Liu, B. Zhang, J. Yao, T. Hayat, A. Alsaedi, S. Dai, ChemSusChem 2018; b) J. Dong, J. Jia, L. Fan, M. Huang, J. Lin, X. He, Z. Lan, ChemSusChem 2017.
[6] a) J. Troughton, K. Hooper, T. M. Watson, Nano Energy 2017, 39, 60-68; b) M. Yin, F. Xie, H. Chen, X. Yang, F. Ye, E. Bi, Y. Wu, M. Cai, L. Han, Journal of Materials Chemistry A 2016, 4, 8548-8553; c) T. Bu, L. Wu, X. Liu, X. Yang, P. Zhou, X. Yu, T. Qin, J. Shi, S. Wang, S. Li, Advanced Energy Materials 2017, 7.
[7] Y. Wang, J. Wu, P. Zhang, D. Liu, T. Zhang, L. Ji, X. Gu, Z. D. Chen, S. Li, Nano Energy 2017, 39, 616-625.
[8] a) B. J. Kim, D. H. Kim, Y.-Y. Lee, H.-W. Shin, G. S. Han, J. S. Hong, K. Mahmood, T. K. Ahn, Y.-C. Joo, K. S. Hong, Energy & Environmental Science 2015, 8, 916-921; b) S. N. Habisreutinger, T. Leijtens, G. E. Eperon, S. D. Stranks, R. J. Nicholas, H. J. Snaith, Nano letters 2014, 14, 5561-5568.
[9] Q. Tai, P. You, H. Sang, Z. Liu, C. Hu, H. L. Chan, F. Yan, Nature communications 2016, 7.
[10] G. Li, T. Zhang, Y. Zhao, Journal of Materials Chemistry A 2015, 3, 19674-19678.
[11] J. Y. Jeng, Y. F. Chiang, M. H. Lee, S. R. Peng, T. F. Guo, P. Chen, T. C. Wen, Advanced Materials 2013, 25, 3727-3732.
[12] a) T. He, Z. Liu, Y. Zhou, H. Ma, Solar Energy Materials and Solar Cells 2018, 176, 280-287; b) H. Tsai, W. Nie, P. Cheruku, N. H. Mack, P. Xu, G. Gupta, A. D. Mohite, H.-L. Wang, Chemistry of Materials 2015, 27, 5570-5576; c) W. Liao, D. Zhao, Y. Yu, C. R. Grice, C. Wang, A. J. Cimaroli, P. Schulz, W. Meng, K. Zhu, R. G. Xiong, Advanced Materials 2016, 28, 9333-9340; d) S. C. Watthage, Z. Song, N. Shrestha, A. B. Phillips, G. K. Liyanage, P. J. Roland, R. J. Ellingson, M. J. Heben, ACS applied materials & interfaces 2017, 9, 2334-2341.
[13] a) S. Sun, T. Salim, N. Mathews, M. Duchamp, C. Boothroyd, G. Xing, T. C. Sum, Y. M. Lam, Energy & Environmental Science 2014, 7, 399-407; b) J.-H. Im, C.-R. Lee, J.-W. Lee, S.-W. Park, N.-G. Park, Nanoscale 2011, 3, 4088-4093; c) T. Baikie, Y. Fang, J. M. Kadro, M. Schreyer, F. Wei, S. G. Mhaisalkar, M. Graetzel, T. J. White, Journal of Materials Chemistry A 2013, 1, 5628-5641.
[14] K.-M. Lee, C.-J. Lin, B.-Y. Liou, S.-M. Yu, C.-C. Hsu, V. Suryanarayanan, M.-C. Wu, Solar Energy Materials and Solar Cells 2017, 172, 368-375.
[15] G. Williamson, W. Hall, Acta metallurgica 1953, 1, 22-31.
[16] a) B. Li, C. Fei, K. Zheng, X. Qu, T. Pullerits, G. Cao, J. Tian, Journal of Materials Chemistry A 2016, 4, 17018-17024; b) Y.-K. Ren, X.-H. Ding, Y.-H. Wu, J. Zhu, T. Hayat, A. Alsaedi, Y.-F. Xu, Z.-Q. Li, S.-F. Yang, S.-Y. Dai, Journal of Materials Chemistry A 2017, 5, 20327-20333.
[17] R. Szostak, J. A. Castro, A. S. Marques, A. F. Nogueira, Journal of Photonics for Energy 2017, 7, 022002.
[18] a) Z. Zhu, V. G. Hadjiev, Y. Rong, R. Guo, B. Cao, Z. Tang, F. Qin, Y. Li, Y. Wang, F. Hao, Chemistry of Materials 2016, 28, 7385-7393; b) X. Guo, C. McCleese, C. Kolodziej, A. C. Samia, Y. Zhao, C. Burda, Dalton Transactions 2016, 45, 3806-3813.
[19] S. Sidhik, D. Esparza, A. Martínez-Benítez, T. López-Luke, R. Carriles, E. De la Rosa, Journal of Power Sources 2017, 365, 169-178.
[20] N. Lin, J. Qiao, H. Dong, F. Ma, L. Wang, Journal of Materials Chemistry A 2015, 3, 22839-22845.
[21] P. Atkins, J. De Paula, J. Keeler, Atkins' physical chemistry, Oxford university press, 2018.
[22] a) H. Rowley, W. R. Reed, Journal of the American Chemical Society 1951, 73, 2960-2960; b) S. Paek, P. Schouwink, E. N. Athanasopoulou, K. Cho, G. Grancini, Y. Lee, Y. Zhang, F. Stellacci, M. K. Nazeeruddin, P. Gao, Chemistry of Materials 2017, 29, 3490-3498.
[23] Y. Rong, S. Venkatesan, R. Guo, Y. Wang, J. Bao, W. Li, Z. Fan, Y. Yao, Nanoscale 2016, 8, 12892-12899.
[24] M. Acik, T. M. Alam, F. Guo, Y. Ren, B. Lee, R. A. Rosenberg, J. F. Mitchell, I. K. Park, G. Lee, S. B. Darling, Advanced Energy Materials 2018, 8.
[25] Y. Zhou, O. S. Game, S. Pang, N. P. Padture, The journal of physical chemistry letters 2015, 6, 4827-4839.
[26] M. K. Kim, T. Jeon, H. I. Park, J. M. Lee, S. A. Nam, S. O. Kim, CrystEngComm 2016, 18, 6090-6095.
[27] K. Wang, Y. Shi, B. Li, L. Zhao, W. Wang, X. Wang, X. Bai, S. Wang, C. Hao, T. Ma, Advanced Materials 2016, 28, 1891-1897.
[28] W. Zhou, P. Zhou, X. Lei, Z. Fang, M. Zhang, Q. Liu, T. Chen, H. Zeng, L. Ding, J. Zhu, ACS applied materials & interfaces 2018, 10, 1897-1908.
[29] W. Ke, G. Fang, Q. Liu, L. Xiong, P. Qin, H. Tao, J. Wang, H. Lei, B. Li, J. Wan, Journal of the American Chemical Society 2015, 137, 6730-6733.

Entry for the Table of Contents (Please choose one layout)

Layout 1:

FULL PAPER

High-quality $MAPbI_3$ perovskite films were achieved by using diethyl ether as an anti-solvent and methanol as an additive prepared in around 50% RH humid ambient air. Planar solar cells fabricated by using this method exhibited the best efficiency of 16.4 %, which is approximately 160 % higher than the devices fabricated by using only diethyl ether anti-solvent.

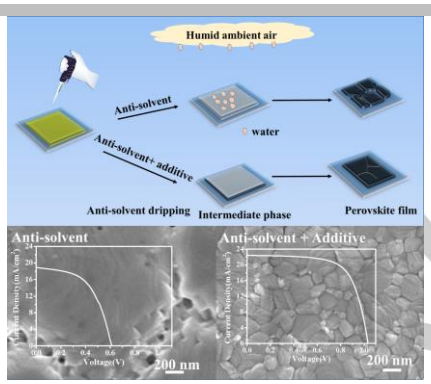

Fu Yang, Muhammad Akmal Kamarudin, Putao Zhang, Gaurav Kapil, Tingli Ma, Shuzi Hayase**

Page 1. – Page 7.

Enhanced Crystallization by Methanol Additive in Anti-solvent for Achieving High-quality $MAPbI_3$ Perovskite Films in Humid Atmosphere

Enhanced Crystallization by Methanol Additive in Anti-solvent for Achieving High-quality $MAPbI_3$ Perovskite Films in Humid Atmosphere

Fu Yang*, Muhammad Akmal Kamarudin, PuTao Zhang, Gaurav Kapil, Tingli Ma, Shuzi Hayase*

Kyushu Institute of Technology, 204 Hibikino Wakamatsu-ku, Kitakyushu 808-0196, Japan

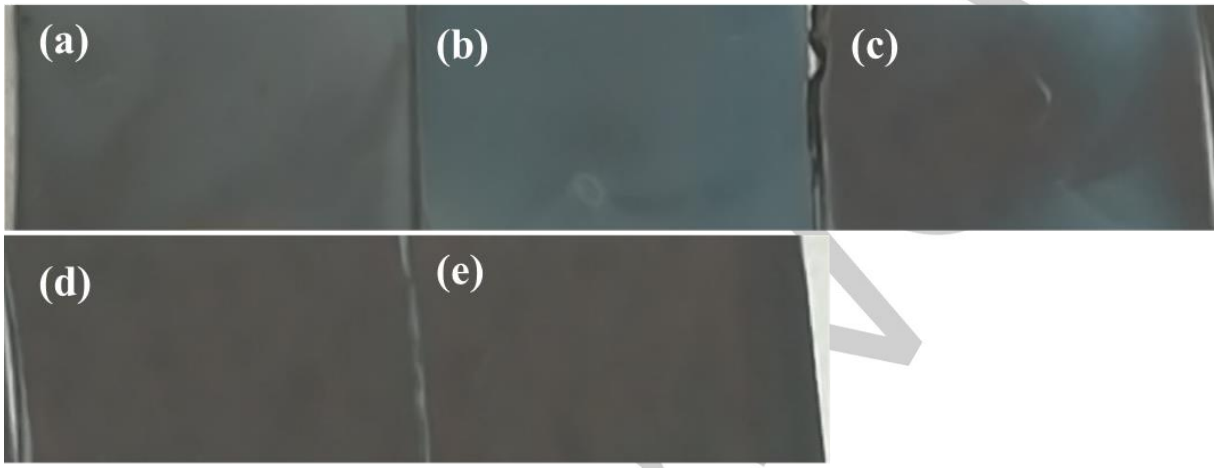

Figure S1 Photographs of $MAPbI_3$ perovskite films of glasses by different methanol additive concentration anti-solvent. (a) 0 %; (b) 1 %; (c) 2 %; (d) 3 %; (e) 4 %.

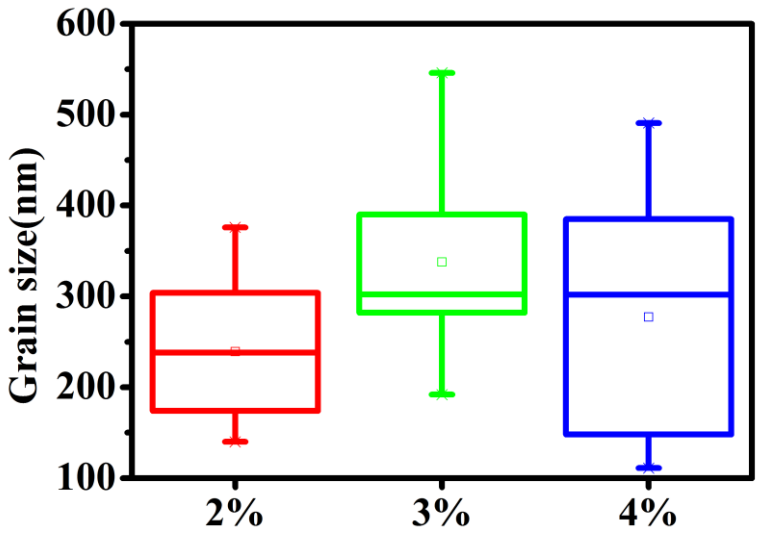

Figure S2 The statistics of grain size based on the SEM image of $MAPbI_3$ perovskite films on FTO glasses prepared by 2%, 3%, and 4% methanol additive anti-solvent.

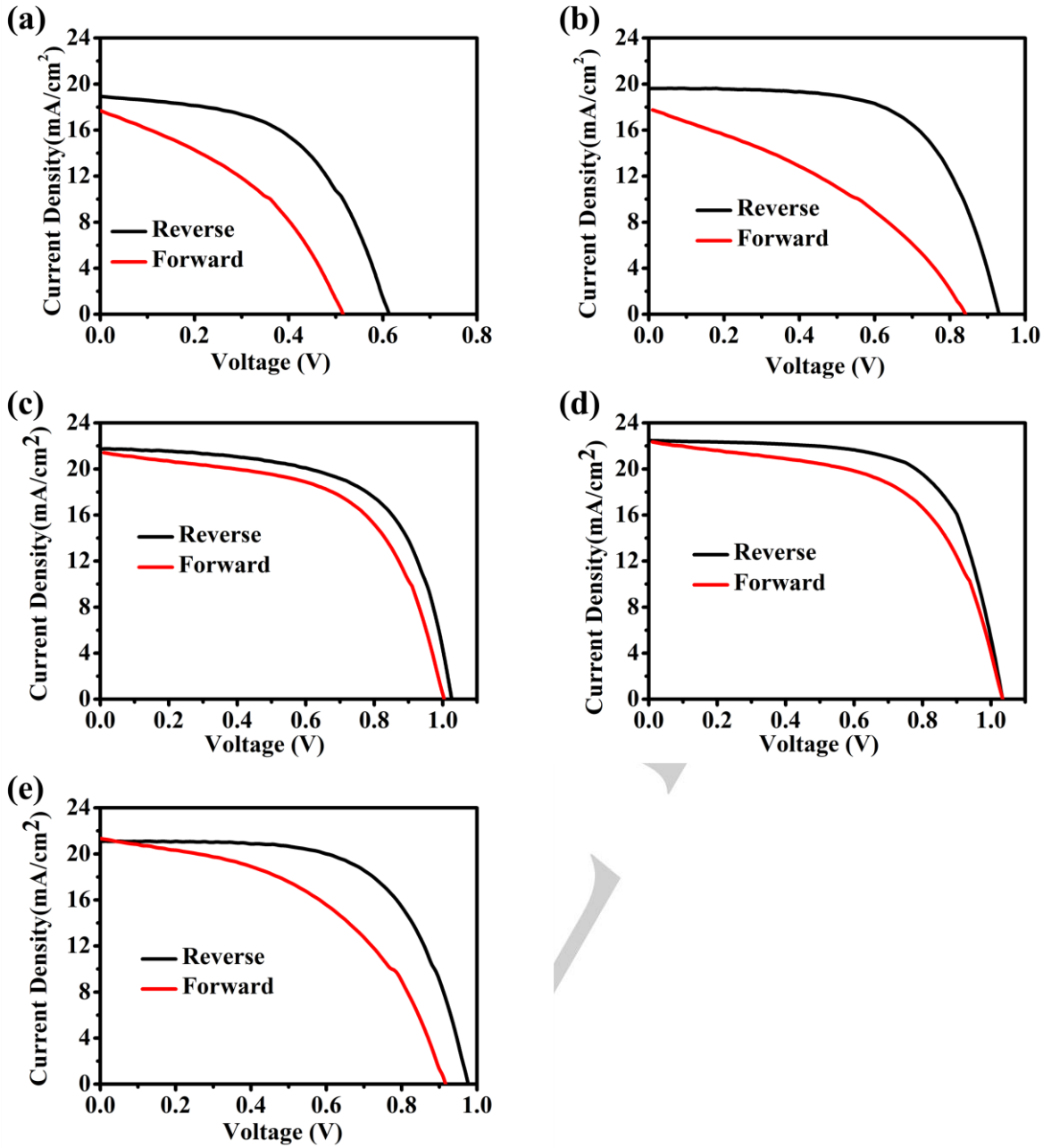

Figure S3 J−V curves of the best-performing $MAPbI_3$ solar cells prepared by different methanol additive anti-solvent under reverse and forward voltage scans. (a) 0 %; (b) 1 %; (c) 2 %; (d) 3 %; (i) (e) 4 %.

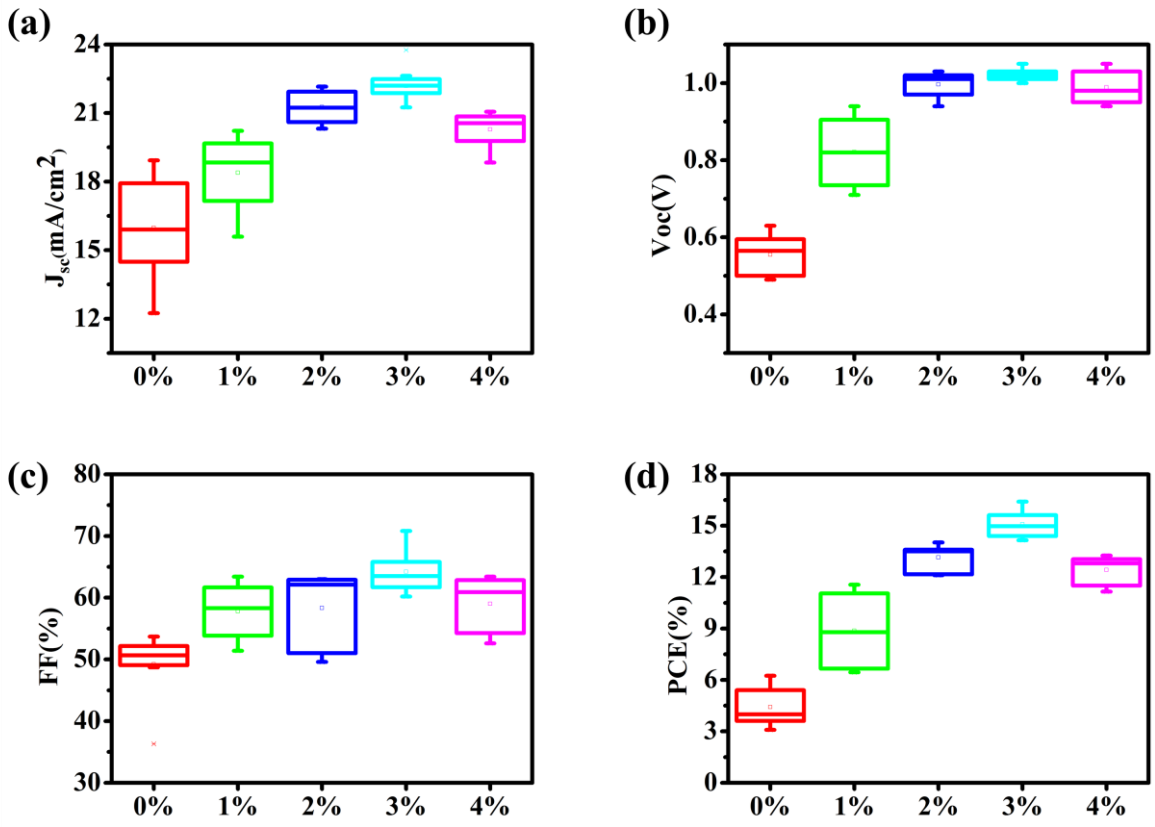

Figure S4 Photovoltaic statistics for the planar perovskite solar cells processed by different methanol additive mixed anti-solvent. (a) J_{SC}, (b) V_{OC}, (c) Fill factor, (d) Efficiency. The boxes represent 40 data from the V_{OC}-to-J_{SC} scan direction.

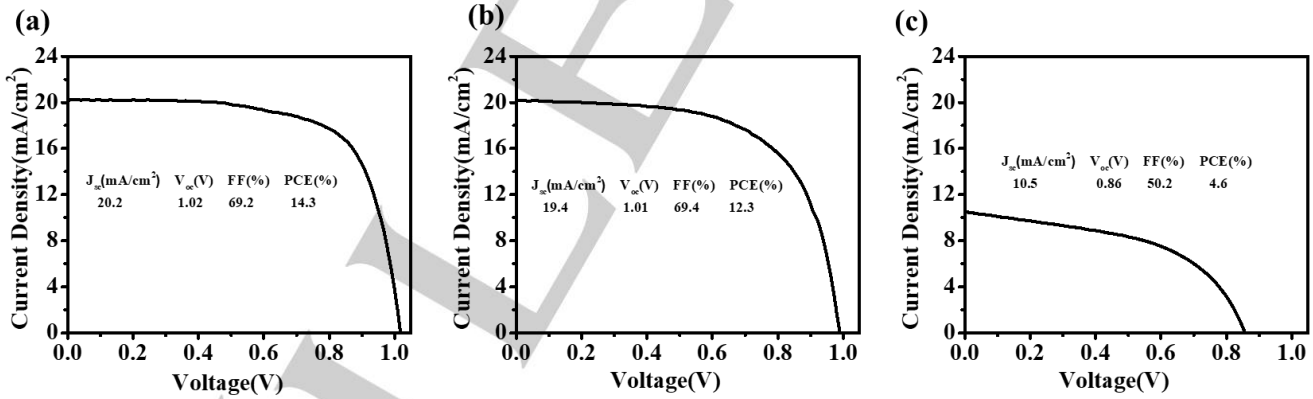

Figure S5 J−V curves of the best-performing $MAPbI_3$ solar cells prepared by different volum ratio water in anti-solvent under reverse scan. (a) 0.5 % water in 3 % methanol additive diethyl ether anti-solvent. (b) 1 % water in 3 % methanol additive diethyl ether anti-solvent. (c) 0.5 % water in diethyl ether anti-solvent.

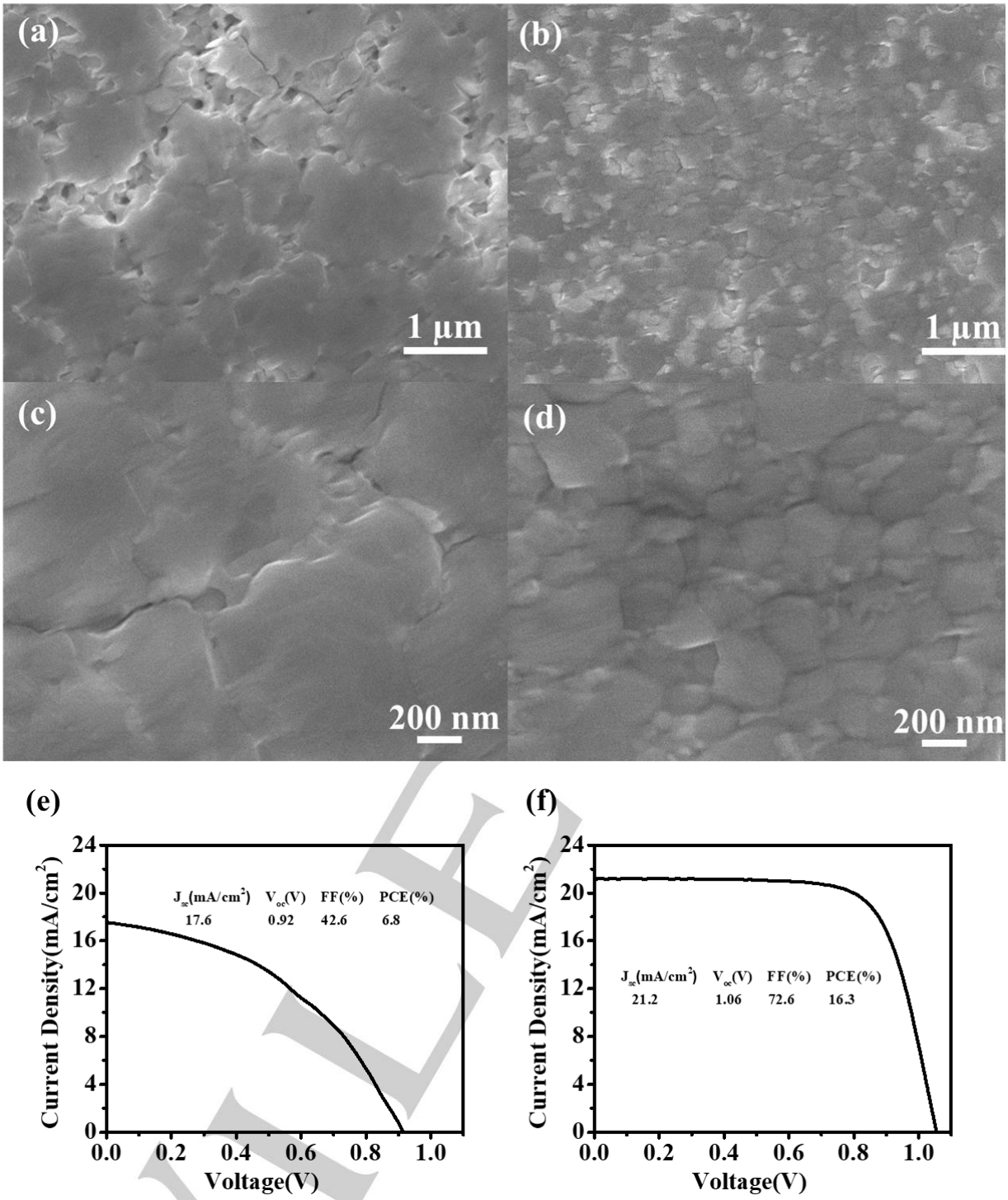

Figure S6 (a) (c) SEM images of $MAPbI_3$ perovskite film prepared by diethyl ether anti-solvent in around 30% RH air atmosphere. (b) (d) SEM images of $MAPbI_3$ perovskite film prepared by 3% methanol additive diethyl ether anti-solvent in around 30% RH air atmosphere. (e) J-V curve of the champion perovskite solar cell prepared by diethyl ether anti-solvent in 30% RH air atmosphere. (f) J-V curve of the champion perovskite solar cell prepared by 3% methanol additive diethyl ether anti-solvent in around 30% RH air atmosphere.

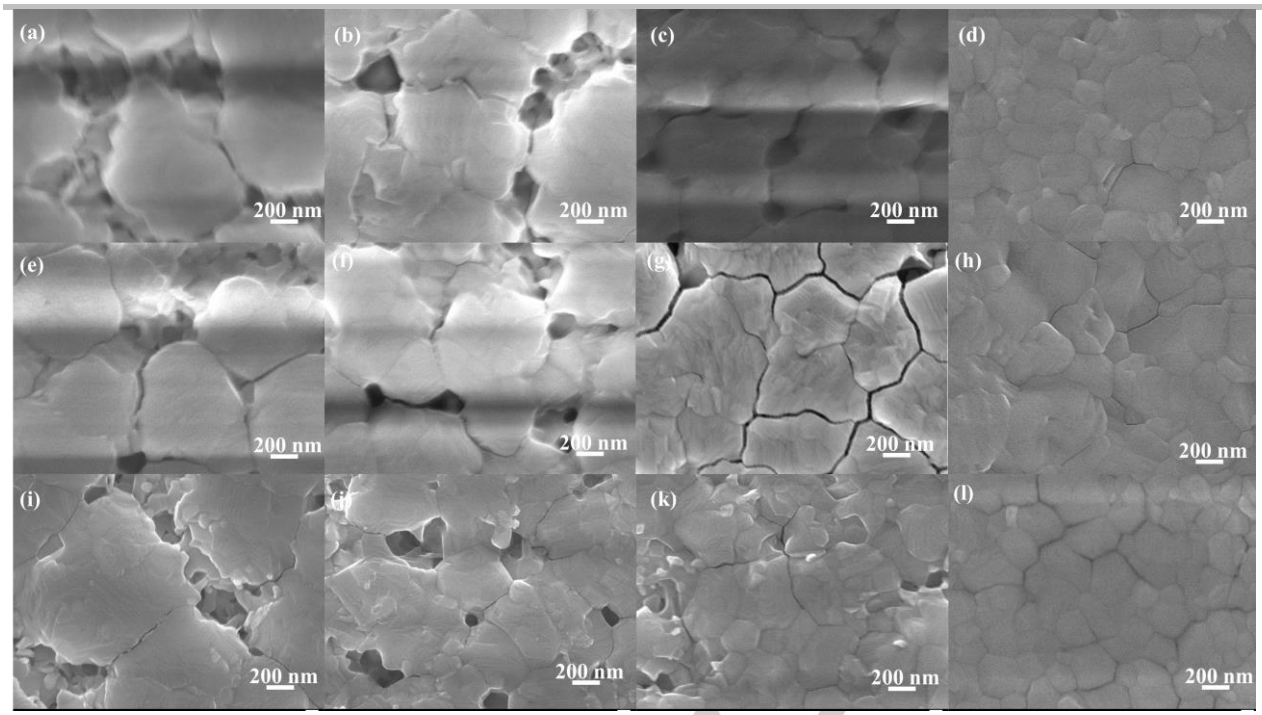

Figure S7 SEM images of $MAPbI_3$ perovskite film prepared by different kind of alcohol additive into diethyl ether anti-solvent. (a) 2% ethanol. (b) 3% ethanol. (c) 4% ethanol. (d) 5% ethanol. (e) 2% 2-propanol. (f) 4% 2-propanol. (g) 6% 2-propanol. (h) 8% 2-propanol. (i) 3% 1-butanol. (j) 6% 1-butanol. (k) 9% 1-butanol. (l) 12% 1-butanol.

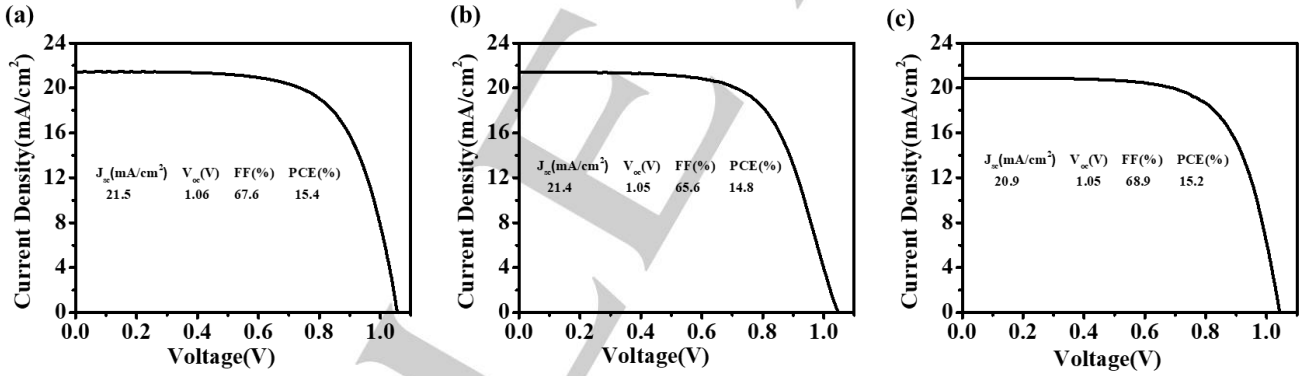

Figure S8 J-V curve of the champion perovskite solar cell prepared by 3% different kind of alcohol additive into diethyl ether anti-solvent. (a) 5% ethanol. (b) 8% 2-propanol (c) 12% 1-butanol.